Supplementary Information

Theoretical Mechanistic Insights into Dinitrogen Activation by a Diniobium Tetrahydride: Two-State Reactivity and the Role of Potassium Cation Promoter

Jimin Yang,[†] Gen Luo,[†,§,*] Yang Yu,[†] Jingping Qu,[†] Zhaomin Hou[†,‡] and Yi Luo[†,*]

[†]State Key Laboratory of Fine Chemicals, School of Chemical Engineering, Dalian University of Technology, Dalian 116024, China

[§]Institutes of Physical Science and Information Technology, Anhui University, Hefei 230601, China

[‡]Organometallic Chemistry Laboratory, RIKEN Cluster for Pioneering Research, and Advanced Catalysis Research Group, RIKEN Center for Sustainable Resource Science, 2-1 Hirosawa, Wako, Saitama 351-0198, Japan

*E-mails: luogen@ahu.edu.cn (G.L.); luoyi@dlut.edu.cn (Y.L.)

Contents:

Table S1. Selected bond distances (Å) and angles (degree) in the optimized $^{1}\mathbf{1}^{K}$ and the X-ray data of $^{1}\mathbf{1}^{K}$ (All hydrogens attached to carbon atom are omitted for clarity)

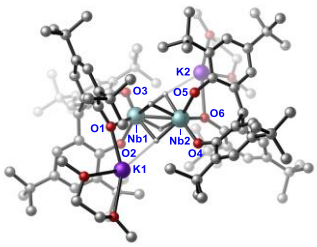

Bond/angle	X-ray	B3LYP/BSI	Δ	B3LYP/BSIII [a]	Δ	B3LYP-D3/BSI	Δ	wB97XD/BSI	Δ
Nb1−Nb2	2.569	2.594	0.025	2.596	0.027	2.561	0.008	2.574	0.005
Nb1−O1	2.056	2.118	0.062	2.055	0.001	2.037	0.019	2.017	0.039
Nb1−O2	2.019	2.092	0.073	2.057	0.038	2.064	0.045	2.045	0.026
Nb1−O3	1.991	2.000	0.009	2.050	0.059	2.021	0.030	2.017	0.026
Nb2−O4	1.991	2.041	0.050	2.002	0.011	2.009	0.018	1.980	0.011
Nb2−O5	2.019	2.065	0.046	2.093	0.074	2.081	0.062	2.071	0.052
Nb2−O6	2.056	2.045	0.011	2.110	0.054	2.123	0.067	2.127	0.071
K1−O1	2.682	2.520	0.162	2.704	0.022	2.691	0.009	2.623	0.059
K2−O6	2.682	2.687	0.005	2.604	0.078	2.502	0.180	2.459	0.223
Average error			**0.049**		**0.040**		**0.049**		**0.057**
Nb1−Nb2−O4	127.05	130.38	3.33	122.82	4.23	118.84	8.21	118.20	8.85
Nb1−Nb2−O5	121.54	118.78	2.76	121.37	0.17	118.09	3.45	117.97	3.57
Nb1−Nb2−O6	119.31	117.81	1.50	114.98	4.33	114.51	4.80	114.06	5.25
Nb2−Nb1−O1	119.31	114.75	4.56	116.73	2.58	130.53	11.22	117.91	1.40
Nb2−Nb1−O2	121.54	118.93	2.61	119.89	1.65	118.66	2.88	113.53	8.01
Nb2−Nb1−O3	127.05	119.84	7.21	130.99	3.94	130.53	3.48	131.38	4.33
Average error			**3.66**		**2.82**		**5.67**		**5.24**

[a] In the BSIII, the 6-31G(d) basis set was used for the atoms in $CHPh_3$ moiety, ^{t}Bu groups and dimethoxyethane (DME) molecule, and the basis sets for other atoms are the same as that in the BSI.

Table S2. Energy comparison (M06/BSII level, kcal/mol) for important species optimized at the B3LYP/BSI and B3LYP/BSIII levels

Method		$^{1}\mathbf{1}^{K}$	$^{1}\mathbf{TS}_{8,9}{}^{K}$ (N−H formation)	$^{1}\mathbf{10}^{K}$	$^{1}\mathbf{TS}_{10,P}{}^{K}$ (2nd H_2 release)
M06/BSII//B3LYP/BSI	ΔG	0.0	30.4	−46.3	−22.4
	$\Delta G^{‡}$		30.4		23.9
M06/BSII//B3LYP/BSIII	ΔG	0.0	30.3	−45.7	−21.6
	$\Delta G^{‡}$		30.3		24.2

Table S3. Calculated energies (M06/BSII//B3LYP/BSI level, kcal/mol) for the dissociation of $[K(DME)]^+$ from complexes $^1\mathbf{1}^{\mathbf{K}}$, $^1\mathbf{6}^{\mathbf{K}}$, $^1\mathbf{8}^{\mathbf{K}}$, $^1\mathbf{9}^{\mathbf{K}}$, and $^1\mathbf{10}^{\mathbf{K}}$

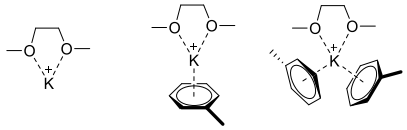

Dissociation equation	ΔG_{sol}
$^1\mathbf{1}^{\mathbf{K}} \rightarrow {}^1\mathbf{1} + 2[K(DME)]^+$	96.5
$2toluene + {}^1\mathbf{1}^{\mathbf{K}} \rightarrow {}^1\mathbf{1} + 2\mathbf{a}$ ($[K(DME)]^+ \cdot toluene$)	102.2
$4toluene + {}^1\mathbf{1}^{\mathbf{K}} \rightarrow {}^1\mathbf{1} + 2\mathbf{b}$ ($[K(DME)]^+ \cdot 2toluene$)	111.1
$^1\mathbf{6}^{\mathbf{K}} \rightarrow {}^1\mathbf{6} + 2[K(DME)]^+$	93.4
$2toluene + {}^1\mathbf{6}^{\mathbf{K}} \rightarrow {}^1\mathbf{6} + 2\mathbf{a}$	99.1
$4toluene + {}^1\mathbf{6}^{\mathbf{K}} \rightarrow {}^1\mathbf{6} + 2\mathbf{b}$	108.1
$^1\mathbf{8}^{\mathbf{K}} \rightarrow {}^1\mathbf{8} + 2\ [K(DME)]^+$	96.8
$2toluene + {}^1\mathbf{8}^{\mathbf{K}} \rightarrow {}^1\mathbf{8} + 2\mathbf{a}$	102.4
$4toluene + {}^1\mathbf{8}^{\mathbf{K}} \rightarrow {}^1\mathbf{8} + 2\mathbf{b}$	111.4
$^1\mathbf{9}^{\mathbf{K}} \rightarrow {}^1\mathbf{9} + 2[K(DME)]^+$	89.7
$2toluene + {}^1\mathbf{9}^{\mathbf{K}} \rightarrow {}^1\mathbf{9} + 2\mathbf{a}$	95.4
$4toluene + {}^1\mathbf{9}^{\mathbf{K}} \rightarrow {}^1\mathbf{9} + 2\mathbf{b}$	104.3
$^1\mathbf{10}^{\mathbf{K}} \rightarrow {}^1\mathbf{10} + 2[K(DME)]^+$	90.9
$2toluene + {}^1\mathbf{10}^{\mathbf{K}} \rightarrow {}^1\mathbf{10} + 2\mathbf{a}$	96.6
$4toluene + {}^1\mathbf{10}^{\mathbf{K}} \rightarrow {}^1\mathbf{10} + 2\mathbf{b}$	105.6

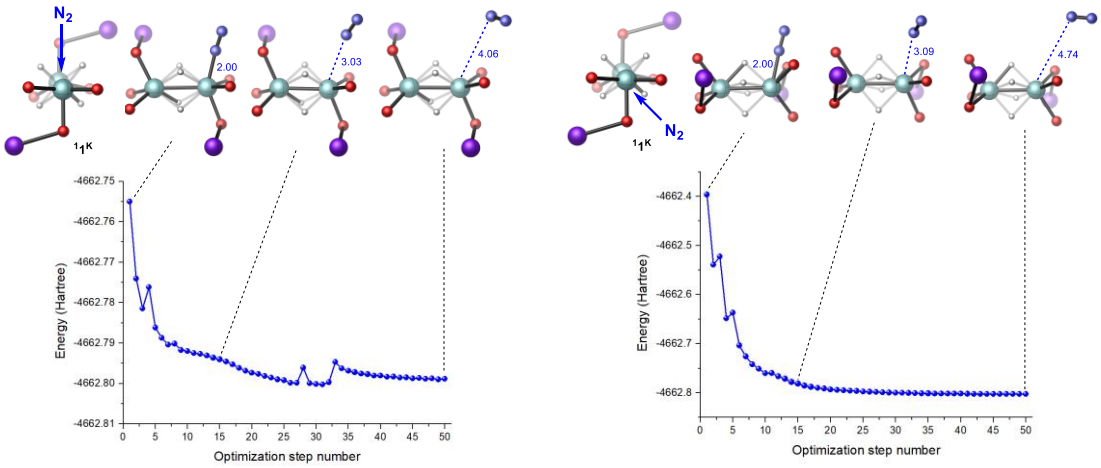

Figure S1. Optimization plot for locating the singlet end-on dinitrogen complex. In the ancillary ligands, only oxygen atoms attached to niobium atoms are shown for clarity. The dinitrogen molecule was eventually found to dissociate form the metal center.

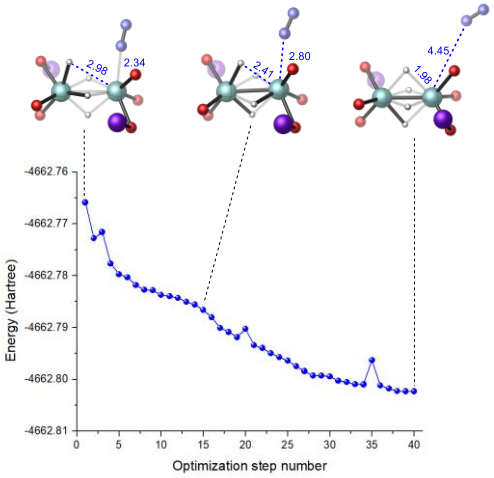

Figure S2. Optimization plot for locating the singlet end-on dinitrogen complex with hydride rearrangement. In the ancillary ligands, only oxygen atoms attached to niobium atoms are shown for clarity. The dinitrogen molecule was eventually found to dissociate form the metal center.

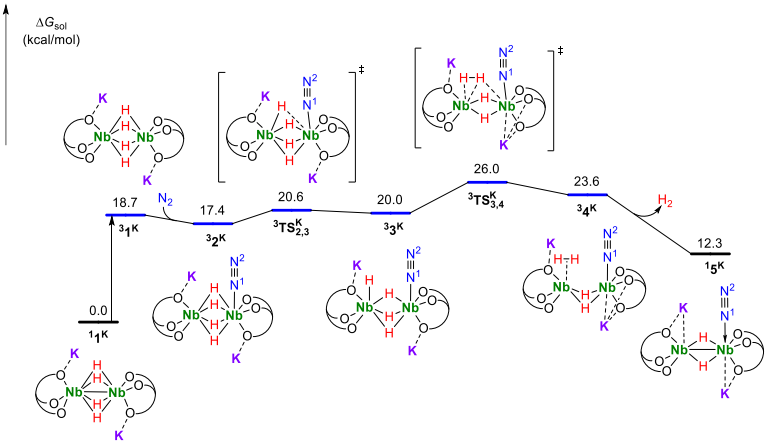

Figure S3. Calculated free energy profile for favorable pathways of N_2 coordination and the first H_2 elimination in $^{1}\mathbf{1}^{\mathbf{K}}$. The left-superscript denotes the spin state of corresponding species.

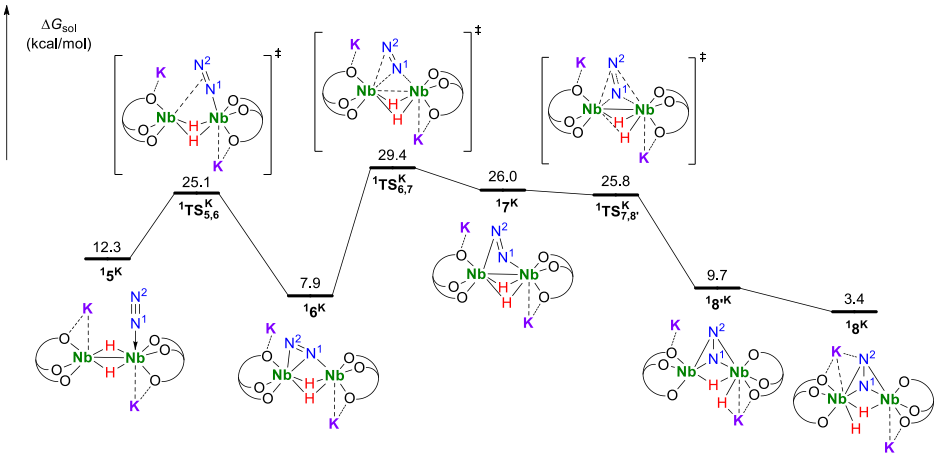

Figure S4. Calculated free energy profile for the favorable pathway of the isomerization of $^{1}\mathbf{5}^{\mathbf{K}}$ to $^{1}\mathbf{8}^{\mathbf{K}}$. The left-superscript denotes the spin state of corresponding species.

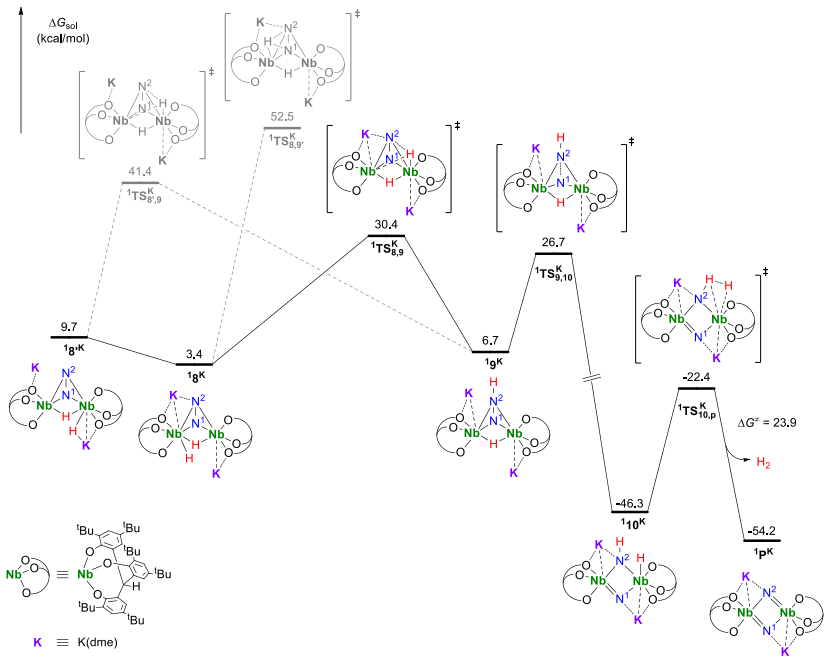

Figure S5. Calculated free energy profile for favorable pathway of the transformation of $^{1}\mathbf{8'^{K}}$ and $^{1}\mathbf{8^{K}}$. The left-superscript denotes the spin state of corresponding species.

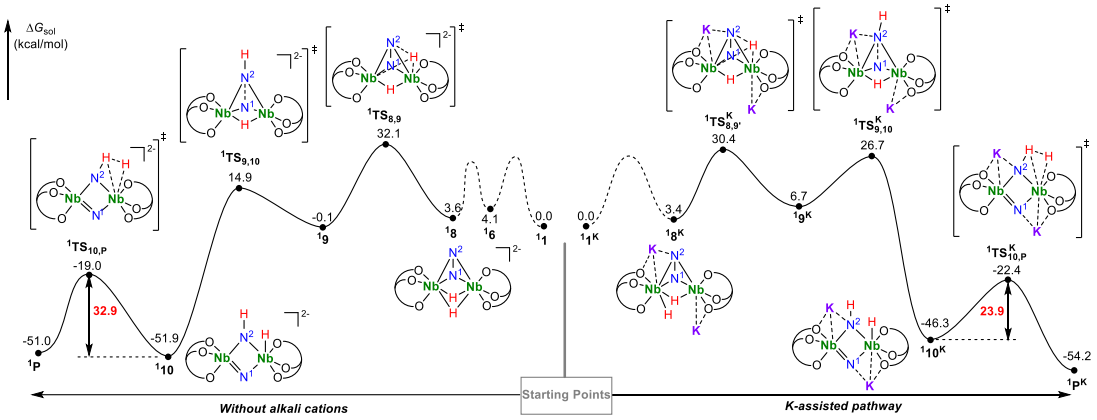

Figure S6. A comparison of energy profile for the anionic $^{1}\mathbf{1}$ and neutral $^{1}\mathbf{1^{K}}$ involved pathways.

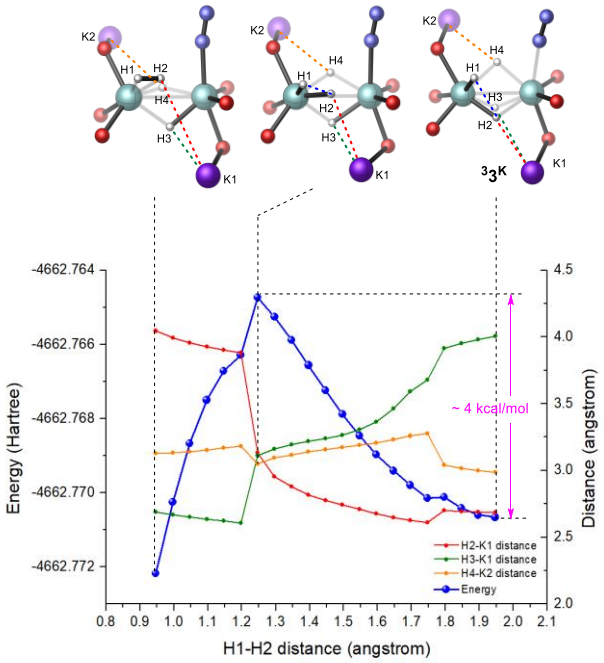

Figure S7. Relaxed PES scan for the H1–H2 distance (step size = –0.05 Å) in ^{3}**3**^{K} at the (U)B3LYP/BSI level.

The relaxed PES scan for the H1–H2 distance in ^{3}**3**^{K} have been performed to investigate the detail process of the first H_2 formation (Figure S7). In the case of ^{3}**3**^{K}, as the H1–H2 distance reduces from 1.95 Å to 0.95 Å, the H2–K1 distance increases from 2.67 Å to 4.05 Å and H3–K1 distance reduces from 4.01 Å to 2.69 Å. While there is much less change in the H4–K2 distance. These results indicate that, during the first H_2 formation, a μ_2-hydride ligand (H2) de-coordinates from K cation to form a terminal hydride ligand. Two terminal hydride ligands (H1 and H2) could form dihydrogen molecule. At the same time, the μ_2-hydride ligand (H3) in ^{3}**3**^{K} coordinates to K cation to stabilize the structure.

Table S4. Energy profile for the transformation of **1**^{K} at various electronic states (energies in kcal/mol)[a]

species	**1**^{K}	**2**^{K}	**TS$_{2,3}$**^{K}	**3**^{K}	**TS$_{3,4}$**^{K}	**4**^{K}	**5**^{K}	**TS$_{5,6}$**^{K}
$S = 0$	0.0	*[b]	*	*	35.3	37.7	12.3	25.1
$S = 1$	18.7	17.4	20.6	20.0	26.0	23.6	13.7	25.9

species	**6**^{K}	**TS$_{6,7}$**^{K}	**7**^{K}	**TS$_{7,8}$**^{K}	**TS$_{8,9}$**^{K}	**9**^{K}	**TS$_{9,10}$**^{K}
$S = 0$	7.9	29.4	26.0	25.8	30.4	6.7	26.7
$S = 1$	13.4	*	*	*	41.5	8.2	26.6

[a] The triplet of Nb(V) species were not considered since there is no *d*-electron on Nb(V) center.
[b] *means the failure in locating the stationary points.

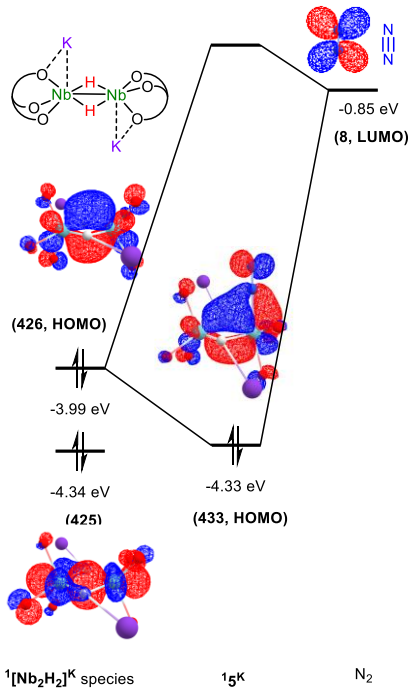

Figure S8. Interaction diagram of frontier molecular orbitals between N_2 moiety and the remained ^{1}**[Nb$_2$H$_2$]^K** species in ^{1}**5^K**. The numbers in parenthesis denote the orbital numbers. In the ancillary ligands, only oxygen atoms attached to niobium atoms are shown for clarity.

Table S5. Imaginary frequency of transition states (*IF*, cm^{-1}), Gas-phase thermal corrections to Gibbs free energy ($\Delta\Delta G_{gas}$, a.u.), and single-point energy (E_{sp}, a.u.) in solution

species	$\Delta\Delta G_{gas}$	E_{sp}	species	$\Delta\Delta G_{gas}$	*IF* (for TS)	E_{sp}
H$_2$	–0.001314	–1.170641				
N$_2$	–0.012851	–109.484618				
^{1}1^K	2.188398	–5734.166116				
^{3}1^K	2.182011	–5734.129853				
^{3}2^K	2.187721	–5843.635168	**^{3}TS$_{2,3}^K$**	2.188342	–158.91	–5843.630718
			^{1}TS$_{3,4}^K$	2.191079	–790.99	–5843.609920
^{3}3^K	2.188518	–5843.631795	**^{3}TS$_{3,4}^K$**	2.188992	–762.69	–5843.622703
^{1}4^K	2.194251	–5843.609322				
^{3}4^K	2.193255	–5843.630849				
^{1}5^K	2.18302	–5842.466614	**^{1}TS$_{5,6}^K$**	2.181302	–8.54	–5842.444564
^{3}5^K	2.181868	–5842.463279	**^{3}TS$_{5,6}^K$**	2.181139	–8.27	–5842.443150
^{1}6^K	2.180694	–5842.472489				
^{3}6^K	2.179698	–5842.461498	**^{1}TS$_{6,7}^K$**	2.179467	–289.46	–5842.435807
^{1}7^K	2.178709	–5842.440486	**^{1}TS$_{7,8'}^K$**	2.177431	–230.63	–5842.439571
^{1}8'^{K}	2.174606	–5842.462357	**^{1}TS$_{8',9}^K$**	2.175531	–1018.13	–5842.412818
^{1}8^K	2.178426	–5842.476281	**^{1}TS$_{8,9}^K$**	2.176845	–1096.64	–5842.431652
			^{3}TS$_{8,9}^K$	2.173251	–936.25	–5842.410397
			^{1}TS$_{8,9'}^K$	2.176316	–830.06	–5842.395891
^{1}9^K	2.184993	–5842.477479	**^{1}TS$_{9,10}^K$**	2.180553	–623.66	–5842.441315
^{3}9^K	2.181675	–5842.471800	**^{3}TS$_{9,10}^K$**	2.177761	–534.86	–5842.438632

^{1}**10**^{K}	2.183613	–5842.560696	^{1}**TS**$_{10,P}$^{K}	2.179723	–1278.00	–5842.518641
^{1}**P**^{K}	2.167076	–5841.384740				
^{1}**1**	1.909952	–3916.847873				
^{1}**6**	1.902039	–4025.158942				
^{1}**8**	1.901842	–4025.159481	^{1}**TS**$_{8,9}$	1.898877	–1084.78	–4025.111104
^{1}**9**	1.905436	–4025.168978	^{1}**TS**$_{9,10}$	1.903050	–632.85	–4025.142707
^{1}**10**	1.906419	–4025.252586	^{1}**TS**$_{10,P}$	1.900464	–1226.41	–4025.194200
^{1}**P**	1.886916	–4024.059717				
^{1}**1**^{Li}	2.149406	–4396.607116				
^{1}**8**^{Li}	2.143249	–4504.924643	^{1}**TS**$_{8,9}$^{Li}	2.139293	–1143.30	–4504.879008
^{1}**10**^{Li}	2.147192	–4505.016191	^{1}**TS**$_{10,P}$^{Li}	2.144828	–1452.47	–4504.969331
^{1}**P**^{Li}	2.128784	–4503.842462				
^{1}**1**^{Na}	2.141882	–4706.099833				
^{1}**8**^{Na}	2.135600	–4814.414221	^{1}**TS**$_{8,9}$^{Na}	2.132194	–1108.76	–4814.367587
^{1}**10**^{Na}	2.139650	–4814.500648	^{1}**TS**$_{10,P}$^{Na}	2.136233	–1317.84	–4814.457978
^{1}**P**^{Na}	2.121579	–4813.321140				
^{1}**1**^{Rb}	2.181575	–4582.466654				
^{1}**8**^{Rb}	2.174139	–4690.780457	^{1}**TS**$_{8,9}$^{Rb}	2.170682	–1097.98	–4690.735367
^{1}**10**^{Rb}	2.176735	–4690.862344	^{1}**TS**$_{10,P}$^{Rb}	2.173994	–1303.70	–4690.823907
^{1}**P**^{Rb}	2.159482	–4689.688016				
^{1}**1**^{Cs}	2.177084	–4574.576233				
^{1}**8**^{Cs}	2.170291	–4682.891428	^{1}**TS**$_{8,9}$^{Cs}	2.166037	–1089.94	–4682.843973
^{1}**10**^{Cs}	2.171771	–4682.969651	^{1}**TS**$_{10,P}$^{Cs}	2.168750	–1302.60	–4682.932888
^{1}**P**^{Cs}	2.155092	–4681.793616				
$[K(DME)]^{+}$	0.117255	–908.560250				
toluene	0.108443	–271.402763				
a	0.237817	–1179.970620				
b	0.365657	–1451.385644				
^{1}**1**^{K}$_{BSIII}$	2.043546	–5734.214591	^{1}**TS**$_{8,9}^{K}_{BSIII}$	2.033199	–1095.51	–5842.481455
^{1}**10**^{K}$_{BSIII}$	2.040241	–5842.609729	^{1}**TS**$_{10,P}^{K}_{BSIII}$	2.036642	–1315.13	–5842.567634
^{1}**10**$_{D3}$	1.918578	–4025.259648	^{1}**TS**$_{10,P\ D3}$	1.912516	–1292.89	–4025.203094
^{1}**10**^{Li}$_{D3}$	2.162901	–4505.024976	^{1}**TS**$_{10,P}^{Li}_{D3}$	2.158502	–1407.64	–4504.980865
^{1}**10**^{Na}$_{D3}$	2.155780	–4814.504995	^{1}**TS**$_{10,P}^{Na}_{D3}$	2.151622	–1349.79	–4814.461473
^{1}**10**^{K}$_{D3}$	2.201001	–5842.573666	^{1}**TS**$_{10,P}^{K}_{D3}$	2.195776	–1305.20	–5842.531675
^{1}**10**^{Rb}$_{D3}$	2.193941	–4690.870716	^{1}**TS**$_{10,P}^{Rb}_{D3}$	2.190334	–1303.13	–4690.836255
^{1}**10**^{Cs}$_{D3}$	2.190809	–4814.504995	^{1}**TS**$_{10,P}^{Cs}_{D3}$	2.186192	–1300.87	–4814.461473
^{1}**10**$_{wB}$	1.945337	–4025.271280	^{1}**TS**$_{10,P\ wB}$	1.938681	–1208.37	–4025.215669
^{1}**10**^{Li}$_{wB}$	2.196420	–4505.035655	^{1}**TS**$_{10,P}^{Li}_{wB}$	2.192553	–1387.90	–4504.991148
^{1}**10**^{Na}$_{wB}$	2.185957	–4814.520030	^{1}**TS**$_{10,P}^{Na}_{wB}$	2.184207	–1331.91	–4814.476718
^{1}**10**^{K}$_{wB}$	2.234302	–5842.588965	^{1}**TS**$_{10,P}^{K}_{wB}$	2.232670	–1344.86	–5842.551592
^{1}**10**^{Rb}$_{wB}$	2.227478	–4690.889921	^{1}**TS**$_{10,P}^{Rb}_{wB}$	2.224718	–1285.03	–4690.853550
^{1}**10**^{Cs}$_{wB}$	2.227389	–4683.002428	^{1}**TS**$_{10,P}^{Cs}_{wB}$	2.225417	–1304.15	–4682.968287

Table S6. The relative free energies (kcal/mol) of the stationary points involved in the N−H formation and the second H_2 elimination in the presence of various alkali cations

Alkali cation	N−H formation			The second H_2 elimination			product
	^{1}**8**	^{1}**TS$_{8,9}$**	$\Delta G^‡$	^{1}**10**	^{1}**TS$_{10,P}$**	$\Delta G^‡$	^{1}**P**
None	3.6	32.1	32.1	–51.9	–19.0	32.9	–51.0
Li(THF)	1.1	27.3	27.3	–53.8	–25.9	27.9	–64.3
Na(THF)	3.0	30.2	30.2	–48.7	–24.0	24.6	–55.3
K(DME)	3.4	30.4	30.4	–46.3	–22.4	23.9	–54.2
Rb(DME)	2.7	28.8	28.8	–47.1	–24.7	22.4	–56.4
Cs(DME)	2.2	29.3	29.3	–45.9	–24.8	21.2	–53.9

Table S7. The charge on dinitrogen unit in intermediates **8** (B3LYP/BSI level) in the presence of various alkali cations[a]

Complex	$Q(N^1)$	$Q(N^2)$	ΔQ^b
^{1}**8**	–0.51	–0.57	0.06
^{1}**8^{Li}**	–0.48	–0.65	0.17
^{1}**8Na**	–0.46	–0.65	0.19
^{1}**8^{K}**	–0.52	–0.65	0.12
^{1}**8^{Rb}**	–0.52	–0.64	0.12
^{1}**8^{Cs}**	–0.51	–0.64	0.13

[a] Mulliken atomic charge. [b] $\Delta Q = Q(N^1) - Q(N^2)$.

Table S8. The relative free energy barrier ($\Delta G^‡$, kcal/mol) and dihedral angle change ($\Delta\varphi$, degree) of Nb1−Nb2−N2−H1 of the stationary points involved in the second H_2 elimination in the presence of various alkali cations optimized by B3LYP-D3 and wB97XD

Alkali cation	M06/BSII//B3LYP-D3/BSI		M06/BSII//wB97XD/BSI	
	$\Delta G^‡$	$\Delta\varphi$	$\Delta G^‡$	$\Delta\varphi$
None	31.7	101.1	30.7	100.5
Li(THF)	24.9	64.7	25.5	65.7
Na(THF)	24.7	66.7	26.1	66.4
K(DME)	23.1	64.8	22.4	58.3
Rb(DME)	19.4	63.3	21.1	61.6
Cs(DME)	18.1	60.4	20.2	59.3

Table S9. The N−N distances (angstrom) and Mulliken charges on the dinitrogen moiety and H1−H2 unit in the intermediates and transition states involved in the transformation of ^{3}**2^{K}** to ^{1}**6^{K}**.

Species	d(N−N)	$Q(N^1) + Q(N^2)$	$Q(H^1) + Q(H^2)$
^{3}**2^{K}**	1.107	0.01	−0.36
^{3}**TS$_{2,3}^{K}$**	1.109	−0.03	−0.36
^{3}**3^{K}**	1.110	−0.05	−0.40
^{3}**TS$_{3,4}^{K}$**	1.119	−0.15	−0.19
^{3}**4^{K}**	1.130	−0.27	0.11
^{1}**5^{K}**	1.129	−0.24	0.00
^{1}**TS$_{5,6}^{K}$**	1.137	−0.33	0.00
^{1}**6^{K}**	1.252	−0.80	0.00